Lab on a Chip

RSC Publishing

PAPER

View Article Online
View Journal | View Issue

Cite this: *Lab Chip*, 2013, **13**, 3578

Liver-cell patterning Lab Chip: mimicking the morphology of liver lobule tissue†

Chen-Ta Ho,[a] Ruei-Zeng Lin,[b] Rong-Jhe Chen,[a] Chung-Kuang Chin,[a] Song-En Gong,[a] Hwan-You Chang,[b] Hwei-Ling Peng,[c] Long Hsu,[d] Tri-Rung Yew,[e] Shau-Feng Chang[f] and Cheng-Hsien Liu*[a]

Received 2nd April 2013,
Accepted 1st May 2013

DOI: 10.1039/c3lc50402f

www.rsc.org/loc

A lobule-mimetic cell-patterning technique for on-chip reconstruction of centimetre-scale liver tissue of heterogeneous hepatic and endothelial cells *via* an enhanced field-induced dielectrophoresis (DEP) trap is demonstrated and reported. By mimicking the basic morphology of liver tissue, the classic hepatic lobule, the lobule-mimetic-stellate-electrodes array was designed for cell patterning. Through DEP manipulation, well-defined and enhanced spatial electric field gradients were created for in-parallel manipulation of massive individual cells. With this liver-cell patterning labchip design, the original randomly distributed hepatic and endothelial cells inside the microfluidic chamber can be manipulated separately and aligned into the desired pattern that mimicks the morphology of liver lobule tissue. Experimental results showed that both hepatic and endothelial cells were orderly guided, snared, and aligned along the field-induced orientation to form the lobule-mimetic pattern. About 95% cell viability of hepatic and endothelial cells was also observed after cell-patterning demonstration *via* a fluorescent assay technique. The liver function of CYP450-1A1 enzyme activity showed an 80% enhancement for our engineered liver tissue (HepG2+HUVECs) compared to the non-patterned pure HepG2 for two-day culturing.

Introduction

Regenerative medicine has an urgent demand for engineered tissues and organs to solve the shortage of tissue source.[1] Over the past two decades, tissue engineering has been of high interest in tissue regeneration but lacks the capability to reconstruct complicated architectures of tissue especially like the liver. A variety of recent progress in tissue engineering has been dedicated to the development of cell-based artificial tissue.[2,3] Cellular patterning techniques, which provide the basis of development for rebuilding cell blocks, play a crucial role in a series of applications such as tissue genetic morphologies,[4,5] medical diagnostics,[6] and drug delivery.[7,8] A functional organ is normally constructed from multiple cell types organized in unique structures to perform its specific and complex functions.[3] Thus, efficient reconstruction of complex tissue structures according to their native morphologies is significant to the *in vitro* development of functional tissue.[9] The efficient reconstruction of complex artificial tissues according to their genetic morphologies, such as liver, highly relies on the fine cellular patterning method. Traditional tissue engineering methods use scaffolds for tissue reconstruction. Although advanced biodegradable scaffolds,[10,11] which morphologically mimic human tissue, have been developed as the cultured matrix for the cell attachment, it is still insufficient to guide, place and distribute the heterogeneous cells to reconstruct complicated architectures of tissue especially like kidney and liver. In particular, hepatic sinusoids, the special micro-vascular systems of the liver which are lined by liver sinusoid endothelial cells to form a radiating pattern, are essential for normal liver function and hepatocyte survival.[12] Thus, fine cell-patterning techniques are important in tissue engineering because the adequate positioning of both hepatic and endothelial cells to reconstruct the complex liver tissue according to its native architecture is the major challenge in liver tissue engineering.[4,5] However, most tissue engineering capabilities deal with relatively simple tissues and fail to arrange heterogeneous cell types to reconstruct the complicated tissues with adequate precision.

Recent advances in passive cell patterning techniques, which focus on chemically modifying cell-adhesive substrate

[a]*Department of Power Mechanical Engineering, National Tsing Hua University, Hsinchu, Taiwan 300, R.O.C.. E-mail: liuch@pme.nthu.edu.tw; Tel: +886-3-5742496*
[b]*Institute of molecular medicine, National Tsing Hua University, Hsinchu, Taiwan 300, R.O.C.*
[c]*Department of Biological Science and Technology, National Chiao-Tung University, Hsinchu, Taiwan 300, R.O.C.*
[d]*Department of Electrophysics, National Chiao-Tung University, Hsinchu, Taiwan 300, R.O.C.*
[e]*Department of Materials Science and Engineering Department, National Tsing Hua University, Hsinchu, Taiwan 300, R.O.C.*
[f]*ITRI, Hsinchu, Taiwan 300, R.O.C.*

† Electronic supplementary information (ESI) available: Videos showing the demonstration of on-chip liver-lobule-mimetic cell patterning. See DOI: 10.1039/c3lc50402f

by photolithography,[13] microcontact printing,[14] and microfluidic patterning,[15] usually require complicated pretreatments and are limited by the intrinsically slow and irregular cellular adhesion. Active cell patterning techniques such as ink-jet patterning[16] and laser-guided writing[17] can handle different cell types, but the patterning resolution and the laser energy loading on cells are still the major concerns. A recent developed technique,[18,19] which uses non-contact cell printing/feeding allowing cell patterning with spatial control and minimization of cell damage, shows promising applications; but the cell-level patterning resolution is still quite away from the desired. Thus, the development of high-resolution cell patterning, which is also capable of rapidly controlling multiple types of cells with good cell viability to preserve cell–cell interactions as well as potentially modulating cell behaviour, is important and challenging.[20]

Compared with the passive cell-patterning techniques addressed above, an active manipulation method, dielectrophoresis (DEP),[21,22] has been recently widely used and demonstrated with the functions of trapping,[23–25] separation,[26,27] sorting,[28,29] and handling[30] for beads, specific bioparticles, and even neural stem cells.[31] For rapid manipulation and patterning on delicate cells like liver cells, our earlier efforts have been demonstrated by taking advantage of negative DEP force for cell patterning and positioning.[20,32] Using negative DEP as the cell-patterning force, which repulses the cells to the region of local electric-field minimum, could reduce the extra energy acting on the cells but a drawback is the cell aggregation in groups, which is unfavourable for clearly forming fine patterns. On the contrary, positive DEP force, which attracts cells to the region of local electric-field maximum, can provide interesting functions such as cell positioning and has been applied to cell registration,[33] living cell arrays[34] and microbial biofilms.[35]

Regarding liver function, the liver plays a central role in drug metabolism. The cytochrome P450 (CYP450) superfamily is a large and diverse group of enzymes, which play a critical role in catalyzing the oxidation of organic substances in the drug metabolism reactions of the liver. The activity of the CYP450 can be characterized as an indicator of liver-specific function to assess the utility for drug metabolism. In this paper, we present a DEP-based cell patterning technique capable of rapid on-chip reconstruction of the large-area pattern of lobule-mimetic liver-tissue with fine patterning resolution and high cell viability, as well as investigate the liver function by examining CYP450-1A1 (Cytochrome P450, family 1, subfamily A, polypeptide 1) activity.

Operating principles and labchip design

Field-induced dielectrophoresis

Dielectrophoresis (DEP) is a phenomenon caused by the induced dipole of polarizable particles in solution under non-uniform electric fields. According to the time-averaged DEP formula,[36] the DEP force F_{DEP} acting on a spherical particle of radius r suspended in a medium with relative permittivity ε_m is

$$F_{DEP} = 2\pi r^3 \varepsilon_m \mathrm{Re}[f_{CM}(\omega)]\nabla E_{rms}{}^2 \quad (1)$$

where E_{rms} is the root mean square of the effective AC electric field. $f_{CM}(\omega)$ is the Clausius–Mossotti factor,[37] which depends on the complex permittivity of both the particle and medium, the conductivity and the angular frequency ω of the applied electric field. $f_{CM}(\omega)$ indicates that the force vector acting on the particle varies with the frequency and depends on the permittivity and the conductivity of the particle and the medium. If $f_{CM}(\omega) > 0$, the particle is more polarizable than the medium. Then the particle is attracted toward the regions of the large electric-field gradient. This is called positive DEP. Contrarily, if the medium is more polarizable than the particle, $f_{CM}(\omega) < 0$, negative DEP force repels the particle toward the region of the local electric-field minimum.

Chip design for lobule-mimetic liver-cell patterning

Liver is considered as a difficult tissue to be reconstructed by tissue engineering due to its complex cellular architecture. The liver contains over a million classical liver lobules. Each lobule is morphologically shaped like a hexagonal plate which consists of hepatocytes radiating from the central vein and being separated by vascular endothelial cells, as illustrated in Fig. 1(a). This unique radiating structure of lobules is essential to make the liver tissue function normally and ensure the optimum nutrient supply and high metabolism reactions exchanging from blood to hepatocytes. To reconstruct heterogeneous cells to mimic the hepatic–endothelial cell-to-cell interaction and the architecture of the specific hexagonal lobule is significant. Our liver-on-a-chip has previously demonstrated the proof-of-concept work to *in vitro* reconstruct the heterogeneous classic lobule of liver tissue with single cell resolution.[20] The cell manipulation mechanism we used for cell patterning is DEP. DEP is a phenomenon caused by the induced dipole of the polarizable particles in the solution under non-uniform electric fields. By appropriately selecting cell type, corresponding medium, and specific electrode geometry design, the positive DEP force can attract polarized cells of homo-type toward the electric-field gradient maximum. We highlight the concept that the control of the electric-field gradient is equivalent to the position control of patterned cells *via* positive DEP manipulation. Following up with this concept, we present here a design of a cell-patterning lab-chip for rapid and *in vitro* reconstruction of centimetre-scale heterogeneous hexagonal lobule-mimetic liver tissue.

Fig. 1(a) illustrates the morphology of one unit of a classic hepatic lobule, which is mainly composed of hepatic cells and liver sinusoid endothelial cells. By mimicking the morphology of liver tissue, the lobule-mimetic-stellate-electrodes array is designed and utilized for liver cell patterning *via* DEP manipulation [Fig. 1(b)]. The radial-shaped 1st (inner) and

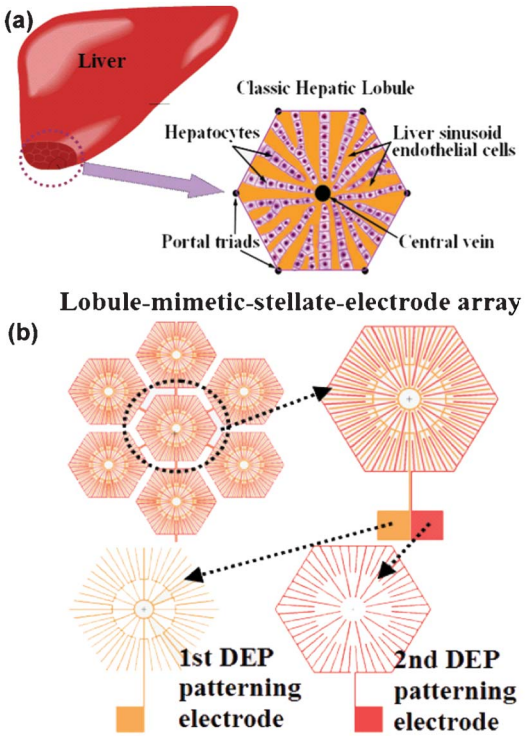

Fig. 1 (a) Illustrated configuration of one basic unit of liver tissue, the classic hepatic lobule. (b) The lobule-mimetic-stellate-electrodes array. Each lobule-mimetic-stellate-electrode consists of two controllable electrodes (1st and 2nd DEP patterning electrodes) for trapping hepatic and endothelial cells, respectively.

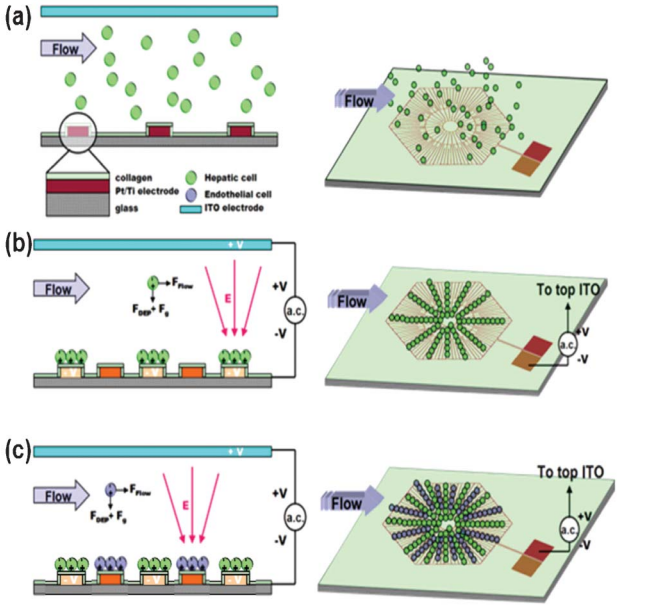

Fig. 2 The configuration and operation principles of DEP-based heterogeneous lobule-mimetic cell patterning. (a) Randomly distributed hepatic cells are loaded into the microfluidic chamber. (b) The hepatic cells are captured and patterned onto the 1st DEP patterning electrodes to form the radial cell-string pattern after the vertical positive DEP voltage is applied. (c) The endothelial cells are, then, loaded, guided and positioned in-between the patterned hepatic cells *via* applying the positive DEP voltage on the 2nd DEP patterning electrode. The heterogeneous integration of hepatic and endothelial cells is performed to mimic the hexagonal lobule of liver tissue.

2nd (outer) DEP patterning electrodes are designed and used to trap hepatic and endothelial cells, respectively. To minimize the number of electrode pads, the inner/outer electrode with centripetal/centrifugal connective design provides two independent controllable electrodes for manipulating two different cell types. Furthermore, the outer part of 1st/2nd cell patterning electrode has a dense electrode design for patterning more cells.

The operation principle of lobule-mimetic cell patterning for heterogeneous hepatic and endothelial cells

Fig. 2(a) illustrates the configuration of the liver-cell patterning labchip and the operation principle of the lobule-mimetic heterogeneous liver cell patterning. The inert platinum electrodes are micromachined above the bottom glass substrate to form the lobule-mimetic-stellate-electrodes array. Top transparent indium-tin-oxide (ITO) glass is used. After the vertical positive DEP voltage is applied on the first cell patterning electrode, hepatic cells are, then, guided, snared, and patterned onto the first lobule-mimetic-stellate-electrodes, as shown in Fig. 2(b). After changing the sucrose medium into culture medium for the cell-to-substrate adhesion of the first hepatic cells, the second type of endothelial cell is loaded into the microfluidic chamber. Then, the vertical positive DEP voltage on the second cell patterning electrode is turned on to trap the endothelial cells onto the desired position. Millions of endothelial cells are captured, patterned, and interlaced in-between the first patterned hepatic cells to achieve the heterogeneous integration of liver-cell patterning, as shown in Fig. 2(c).

Materials and methods

Microfabrication process

The liver-cell patterning labchip was micromachined using the Integrated Circuit (IC) photolithography process which is summarized and illustrated in Fig. 3(a)–(d). A bare glass wafer was cleaned using the piranha technique. The patterns of lobule-mimetic-stellate-electrodes were defined on the glass wafer using a photolithography process. This was followed by depositing a metal layer of 200 Å/2000 Å titanium/platinum *via* E-Gun evaporation. Then, the fine geometric patterns of the lobule-mimetic-stellate-electrodes were transferred onto the glass substrate *via* the lift-off process [Fig. 3(a)]. Prior to packing the whole chip, a thin film of collagen was coated on the bottom glass substrate to enhance the cell-to-substrate adhesion for liver cell patterning [Fig. 3(b)]. Then, a 200 μm thick silicon tape, serving as the spacer, was bound with the patterned glass substrate to form the microfluidic chamber [Fig. 3(c)]. A transparent indium-tin-oxide (ITO) glass, which acted as the top DEP ground electrode, was drilled through *via* a laser bombarding machine to open the inlet/outlet for fluidic

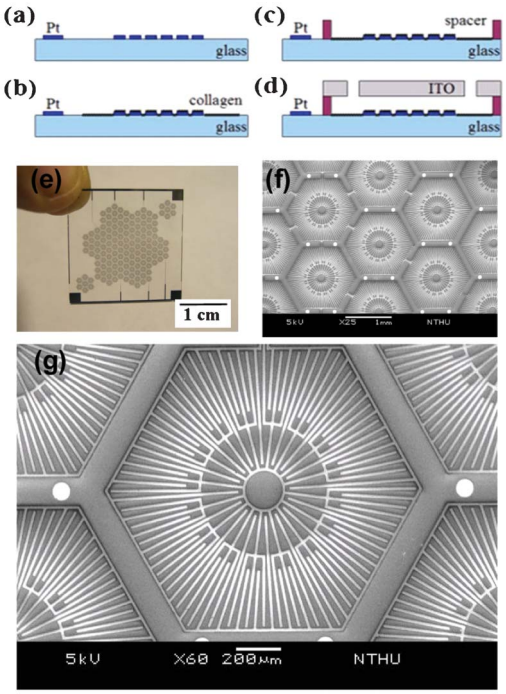

Fig. 3 The microfabrication process and the chip pictures. (a)–(d) summarize the micromachining process. (e)–(g) show the pictures for microfabrication results.

transportation. Right after connecting the plastic tubes to the fluid accesses of the ITO glass, the top ITO glass was bonded with the bottom DEP glass substrate to form the final liver-cell patterning labchip [Fig. 3(d)]. Fig. 3(e)–(g) show a picture of the liver-cell patterning biochip with the dimensions of 25 mm × 25 mm and the SEM zoom-in pictures of the lobule-mimetic-stellate-electrode array.

Cell culture and media

Human liver cell line, HepG2 (ATCC, HB8065), was maintained at 37 °C with 95%/5% air/CO_2 in Dulbecco's modified Eagle's medium (DMEM, Invitrogen, Carlsbad, CA) containing 10% (v/v) heat-inactivated fetal bovine serum (FBS, Biological Industries, Israel) and antibiotics (100 U ml^{-1} penicillin and 100 U ml^{-1} streptomycin, Sigma-Aldrich Co., MO). Human umbilical vein endothelial cells (HUVECs) were prepared as previously described[38] and maintained in EGM-2 medium supplemented with low serum growth supplement at 37 °C with 95%/5% air/CO_2. These two types of cells are utilized to demonstrate the rapid on-chip lobule-mimetic cell patterning of heterogeneous cells in this paper.

Cell preparation for DEP manipulation

Prior to the on-chip cell-patterning demonstration, HepG2 and HUVEC cells were harvested from sub-confluent cultures, detached using 0.2% trypsin (Sigma) with 1 mM EDTA (Sigma) in PBS and re-suspended in the DEP-manipulating sugar medium (8.5% sucrose, 0.3% dextrose and 10 mM HEPES in ddH_2O; conductivity: 80 μS cm^{-1}) to result in a final concentration of 5 × 10^6 cells ml^{-1}. The conductivity of the DEP-manipulating sugar medium was measured *via* a digital conduct meter (330i, WTW, Germany). In cell-patterning demonstrations, HepG2 and HUVEC cells were pre-labelled with biocompatible fluorescent dyes CM-FDA or DiO for green fluorescence and SNARF-1 or DiI for red fluorescence according to the manufacturer's protocols (Molecular Probes, Eugene, OR), which were identified at the excitation/emission wavelengths of 549/565 nm *via* a fluorescent microscope (BX51, Olympus, Tokyo, Japan). Cells were immediately used for DEP-based cell-patterning experiments.

Surface modification of the cell-patterning chamber for cell-adhesion enhancement

To improve the cell-to-substrate adhesion, Type I collagen was used as ECM and cell-adhesion promoter coated on the biochip substrate. The surface modification process began *via* sterilizing the cell-patterning biochip with 70% ethanol for 10 min and drying. Then, the biochip was dipped in a solution of Type I collagen (Sigma, St Louis, MO, USA) with a concentration of 30 μl ml^{-1} at 37 °C for 30 min to adsorb a thin layer of collagen upon the cell patterning area. This was followed by washing the biochip with ddH_2O to ensure that no residues of unbound collagen released on the chip and influenced the cell-patterning condition.

Cell adhesion, growth and viability assessment in the cell-patterning chamber

A programmable adjustment of liquid environment for the cell-patterning chamber was performed carefully as described below to satisfy the different requirements of medium compositions at each step:

STEP I. Cell positioning -

Cells were positioned on chip in parallel *via* positive DEP manipulation with the low-conductive DEP-manipulating sugar buffer under the conditions of a flow rate of 60 μl min^{-1} and an applied DEP voltage of AC 5 V_{pk-pk} at 1 MHz. After the desired cell pattern was formed, the inlet fluid was then switched to pure DEP-buffer without cells with the flow rate increased to 200 μl min^{-1} for 5 min to flush away the extra off-pearl-chain-line cells on the patterning region.

STEP II. Cell adhesion -

Then the DEP-manipulating sugar buffer supplemented with 5 mM Ca^{2+} and 5 mM Mg^{2+} ($\sim$28 mS m^{-1}) was injected to entirely replace the formerly-input DEP-manipulating sugar buffer inside the microfluidic chamber under the conditions of a flow rate of 30 μl min^{-1} for 5 min. Calcium and magnesium were used to enhance the primary cell-to-substrate adhesion. Microfluidic pumping was then turned off for another 5 min to keep the flow stationary and to achieve the primary adhesion of cells to the chip substrate for the following cell culture.

STEP III. Cell growth -

Finally, the whole medium in the cell-patterning chamber was replaced with DMEM medium (5 mM Ca^{2+} and 5 mM Mg^{2+}) *via* pumping injection under the flow rate of 20 μl min^{-1} for 10 min. The bio-chip with patterned cells was then transferred into a CO_2 incubator and maintained under the normal conditions for long-tern cell culturing.

Cell viability assay

The viability/cytotoxicity assays of fluorescein diacetate/ethidium bromide staining (FDA/EtBr: Sigma) were used to assess the health of HepG2 cells by simultaneously distinguishing the living cells from the dead cells *via* the FDA/EtBr dye. FDA dye is highly lipophilic material and readily passes through the plasma membrane of a cell; its acetyl ester groups are then cleaved by intracellular esterase activity to generate fluorescein. EtBr passes through the porous membranes of dead cells and binds to nuclear DNA, which stains the dead cell nuclei red. In the cell viability studies, the HepG2 cells were harvested from sub-confluent cultures, detached using trypsin–EDTA in PBS and centrifuged for 5 min. The trypsinized HepG2 cells were stained by directly adding 10 μg ml^{-1} FDA and 40 μg ml^{-1} EtBr in PBS, re-suspended in the DEP-manipulating sugar buffer and immediately used for the following cell survival experiments.

CYP450-1A1 enzyme activity assay

CYP450 enzyme activity is a liver-specific function to quantitatively assess the drug metabolism of liver cells. The drug metabolism reactions of the liver simply divide into two phase, Phase I and Phase II. During Phase I reactions, a pharmaceutical substance is either introducing a new functional group (*e.g.* hydroxylation) or modifying an existing functional group (*e.g. O*-dealkylation), which results in a more polar metabolite of the original substance. Then, Phase II conjugation reactions involve the interactions of the more polar functional groups of phase I metabolites. Finally, the conjugated metabolites are more soluble in the water and facile excretion. The CYP450 superfamily is a large and diverse group of enzymes, which play a critical role in catalyzing the oxidation of organic substances in Phase I. Therefore, the activity of the CYP450 can be characterized as an indicator of liver-specific function to assess the utility for drug metabolism.

Here CYP450-1A1 enzyme activity was measured by using a modification of the ethoxyresorufin-*O*-deethylase (EROD) assay[39] in our studies. EROD activity describes the rate of the CYP450-1A1-mediated *O*-deethylation of the substrate ethoxyresorufin (ER) to form the product resorufin (fluorescent substance). The catalytic activity towards the ER is an indication of the amount of enzyme present and is quantitated by the fluorescence intensity of produced resorufin in our studies.

The assay medium consisted of 10 μM 7-ethoxyresorufin and 25 μM dicumarol.[40] The 7-ethoxyresorufin, a substrate of the CYP450-1A1 enzyme, was used to measure the CYP450-1A1 enzyme activity of HepG2 and prepared as a 10 mM stock solution in dimethyl sulfoxide (DMSO). When 7-ethoxyresorufin reacts with CYP450-1A1 enzyme in the liver cells, resorufin is generated. Besides, dicumarol, an inhibitor of DT-diaphorase,[41] here was added to retard further metabolism of resorufin into non-fluorescent compounds and prepared as a 10 mM stock solution in NaOH. The final assay medium was dissolved in serum-free DMEM.

Results and discussion

The parameter setup for DEP operation and DEP characterization

Prior to the cell-patterning experiments, both HepG2 cells and HUVECs (10 ~ 12 μm in diameter) were tested to evaluate the frequency domain of the AC signal applicable for the DEP manipulation. First, the sugar buffer with HepG2 cells was loaded into the microfluidic chip *via* the syringe pump. Initially the HepG2 cells were randomly distributed over the cell-patterning chamber. Then, AC potentials with the amplitude increasing from 1 V to 10 V and the frequency varying from 1 Hz to 10 MHz were applied to observe the positive/negative DEP phenomenon.

While operating at 1 V AC bias between the top ITO ground electrode and the bottom lobule-mimetic cell patterning electrode with the entire testing frequency spectrum, HepG2 cells were randomly distributed to show that not enough field-induced DEP force was generated. The DEP effect appears when the input AC bias was increased to 3 V with a generated field intensity of about 30 kV m^{-1}. Experimental results showed that the field-induced negative DEP of HepG2 cells appeared at sub-kHz low-frequency electric field, while the positive DEP was generated at sub-MHz high frequency electric field. The crossover frequency took place at about 15 kHz. Besides, HUVECs exhibit similar DEP manipulation characterization. Moreover, while operating at an AC potential of above 5 V, the frequency should be kept at above 10 kHz to avoid the annoying side-effects of pH variations and gas bubbles caused by the electrochemical electrolysis reaction. After long-term DEP and cell-viability experiments for HepG2 cells and HUVECs, we compromised between the strong DEP force and the good cell viability during/after the DEP manipulation to set up the DEP potential of 5 V_{pk-pk} at 1 MHz with the gentle low-conductivity medium described above to relax the environmental stress for cells.

On-chip in-parallel cell-patterning demonstration and on-chip culturing of patterned liver cells

An on-chip in-parallel cell-patterning demonstration is shown in Fig. 4. First, the fluidic network was prudently filled up with isotonic DEP buffer to avoid bubbles trapped inside the microchamber [Fig. 4(a)]. After DiI-stained HepG2 cells were pumped in (flow rate: 20 μl min^{-1}) and randomly distributed over the cell-patterning area [Fig. 4(b)], the AC potential of 5 V at 1 MHz was biased between the top ITO ground electrode and the bottom lobule-mimetic-stellate-electrode array. The positive DEP force traps the polarized HepG2 cells. The overall resultant forces, with contributions from the field-induced vertical positive DEP force, hydrodynamic drag force, sedimentation force and the gravity force, speeded up guiding the HepG2 cells to the region of electric field maximum. At this stage, the location of the energized lobule-mimetic-stellate electrode provided the spatial local maximum of the electric-field gradient and acted as the primer for positioning the field-guiding cells. HepG2 cells were first trapped in-parallel and accumulated to form a cell cluster at the bottom lobule-mimetic-stellate electrode. After continuous feeding with fresh

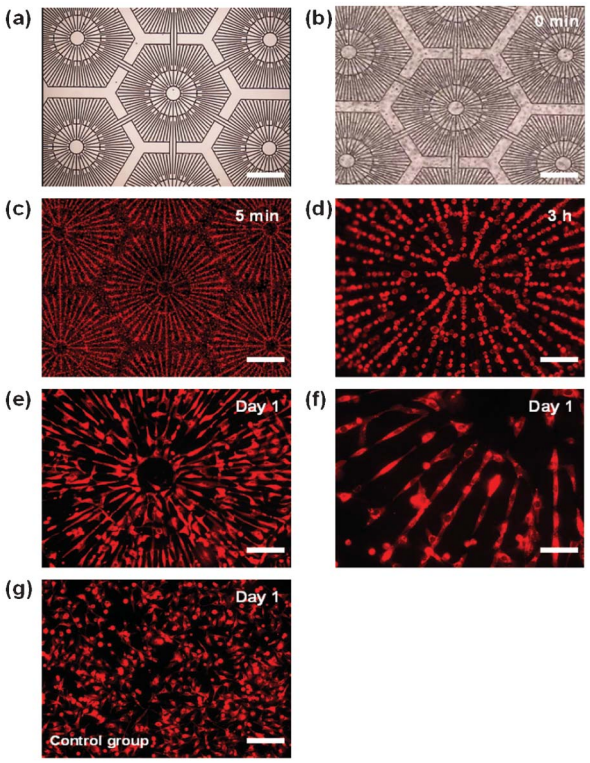

Fig. 4 On-chip and in-parallel DEP-based cell patterning demonstration. (a) White-light snapped OM picture shows the top view of the lobule-mimetic-stellate electrode inside the cell-patterning chamber. (b) Bright-field picture shows the HepG2 cells were randomly distributed after the HepG2 cells were pumped into the cell patterning chamber. (c) After applying an AC potential of 5 V_{pk-pk} at 1 MHz, the red-stained HepG2 cells were in-parallel guided, snared and micropatterned onto the lobule-mimetic-stellate electrode to form the HepG2 cells-assembled pattern. (d) Primary cell-to-substrate adhesion of the HepG2 cells was achieved after three-hour cell culturing. (e) After one-day culturing, the micropatterned HepG2 cells adhered and spread onto the lobule-mimetic-stellate electrode to form the pattern of a multiple radial line array. (f) The enlarged view shows the micropatterned HepG2 cells after one-day culturing. The micropatterned HepG2 cells adhered to the substrate, elongated their body, and spread onto the lobule-mimetic-concentric ring electrodes. (g) HepG2 cells were randomly distributed after one-day culturing without DEP micropatterning, which acted as a control group. Scale bar: (a–c) 500 μm, (d, e, g) 100 μm, (f) 20 μm.

cells coming from the surrounding buffer, the first patterned cells were connected with the incoming cells and vertically piled up. Locally, the length of the cell chain rapidly increased one-by-one with time by the effect of the enhanced field-induced DEP-guiding force. Globally, plenty of cell-chains, then, were organized in place to form the radial pearl-chain array oriented and piled up along the electric field direction starting from the bottom lobule-mimetic-stellate electrode to the top ITO counter electrode. After DEP-based cell patterning had operated for about 5 min, tens of thousands of HepG2 cells were guided, snared and positioned onto the lobule-mimetic-stellate-electrode array to form the large-area and ordered pattern of a hexagon-shaped lobule-mimetic pattern array [Fig. 4(c)]. While the desired cell pattern was formed, a step-by-step medium regulation process was implemented to enhance the cell–substrate adhesion. Then, the whole chip with the DEP-micropatterned cells was then transferred into a CO_2 incubator and cultured under the standard cell culture conditions.

After three hours incubation [Fig. 4(d)], the micropatterned HepG2 cells were in place and the pattern is pretty clear as compared with Fig. 4(c). Some HepG2 cells started to spread their shape which could be seen *via* the morphological change against the non-spreading micropatterned HepG2 cells. Primary cell-to-substrate adhesions in some HepG2 cells were established. After one-day culturing, the micropatterned HepG2 cells maintained in place and grew well, as shown in Fig. 4(e). Compared with the control group of HepG2 cells without DEP cell patterning after one-day culturing [Fig. 4(g)], the DEP micropatterned HepG2 cells showed an excellent result of formation of a high precision pattern. Moreover, the HepG2 cells also adhered and spread onto the substrate to form the pattern of a radial shaped line array of lobule-mimetic pattern. Most of the HepG2 cells adhered and elongated their body along the place of the lobule-mimetic-stellate electrode. This was an interesting phenomenon. This evidence showed that the lobule-mimetic-stellate electrode not only provided the positioning ability for DEP manipulation but also made the topologically micropattern favorable for cell adhesion. This superior characterization also presented a great help to both ensure and enhance the cell patterning resolution.

Cells always showed their normal behavior such as cell motility and migration while they received certain signals in their surrounding environment or they decided to move by themselves. In some regions, two adjacent patterned HepG2 cells were contacted with each other; the boundary between two HepG2 cells was not clear and showed overlapped. In some cases, two HepG2 cells merged into one cellular unity, while somewhere there were more than three or four cells intimately contacted to form a cell group, as shown in Fig. 4(e). Communications between cell–cell and cell–ECM were on-going. Fig. 4(f) shows the enlarged local-view of the DEP micropatterned HepG2 cells. The detailed circumstances of cell adhesion of HepG2 cells could be clearly observed. The HepG2 cells elongated their body and connected one-by-one *via* extending their cytoskeleton to the substrate. The radial straight line pattern of HepG2 cells showed the excellent patterning result *via* our design. Furthermore, the behaviors of cell adhesion, spreading and growth provided the evidence that the DEP-patterned HepG2 cells were not only viable but also revealed their physiological behavior such as, cell-to-cell or cell-to-ECM interactions and cell migration for providing the opportunity to approach functional engineered liver tissue.

In situ cell-viability assessment for DEP cell patterning

The cell viability was assessed with the fluorescein diacetate/ethidium bromide (FDA/EtBr) viability/cytotoxicity assay. The live and the dead cells can be monitored and distinguished simultaneously *via* this FDA/EtBr cell-viability assay method, as shown in Fig. 5. HepG2 cells were micropatterned and aggregated together to form the radial aligned pearl-chain pattern along the location of the lobule-mimetic-stellate-electrode under the DEP operation of 5 $V_{peak-peak}$ at 1 MHz.

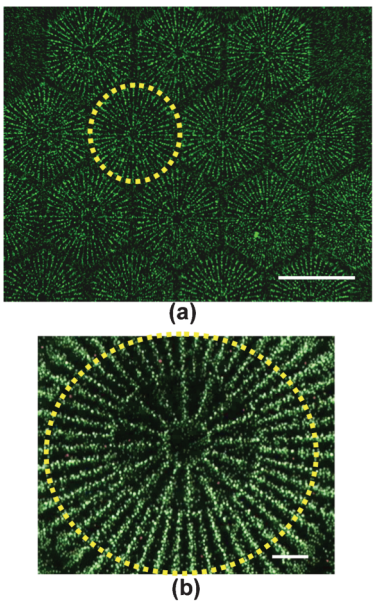

Fig. 5 *In situ* cell-viability assessment for the DEP cell patterning. The fluorescent image for *in situ* FDA/EtBr cell-viability assay shows the viable HepG2 cells (green fluorescence) and the dead HepG2 cells (red fluorescence), respectively. The 95% cell viability of green live hepatic cells is observed after DEP-based cell patterning. Scale bar: (a) 2 mm, (b) 100 μm.

Fig. 5 was recorded after the DEP sugar buffer of 20 μl min^{-1} flow rate (without cells) became steady and flushed away the extra cells out of the cell-patterning chamber under the continuous DEP operation. The experiment results show that the DEP force can trap and hold liver cells against the flow rate up to about 200 μl min^{-1}. After the above DEP operation on liver cells continued for 5 min, the FDA/EtBr dyes were injected into the cell-patterning chamber from the inlet. The fluorescent image for the *in situ* FDA/EtBr cell-viability assay shows the viable HepG2 cells (green fluorescence) and the dead HepG2 cells (red fluorescence), respectively. The 95% cell viability of green live hepatic cells is observed after DEP-based cell patterning.

Centimetre-scale liver-lobule-mimetic reconstruction of heterogeneous HepG2 cells and HUVECs

To approach the *in vitro* lobule-mimetic reconstruction of the classical lobule of liver tissue for the development of functional complex liver tissue, heterogeneous integration of the human liver cells (HepG2) and the human umbilical vein endothelial cells (HUVECs) were organized and demonstrated. However, HepG2 cells and HUVECs possess similar dielectric properties. This made the heterogeneous integration of hepatic and endothelial cells challenging from the engineering aspect. To resolve this issue, the first group of cells needed to be positioned, and adhered to substrate to ensure their normal cellular functions then the second group of cells were micropatterned to achieve the heterogeneous integration. Moreover, to avoid over-proliferation and motility of the micropatterned cells and reserve the good pattern of early settling cells, the heterogeneous integration of hepatic and endothelial cells was performed after the hepatic cells were micropatterned first and cultured for six hours. We did observe some non-specific binding of HepG2 cells to the surface of the 2nd DEP patterning electrode during the first DEP patterning step. Most HepG2 cells of non-specific spreading beyond the 1st patterned electrode could be easily washed away *via* the medium flow.

Fig. 6 shows on-chip heterogeneous-integration demonstration of liver cells (HepG2 cells, red fluorescence) and endothelial cells (HUVECs, green fluorescence) *via* our liver-cell patterning labchip. Fig. 6(a) and (b) show the top-view pictures above the cell-patterning area, before and after the

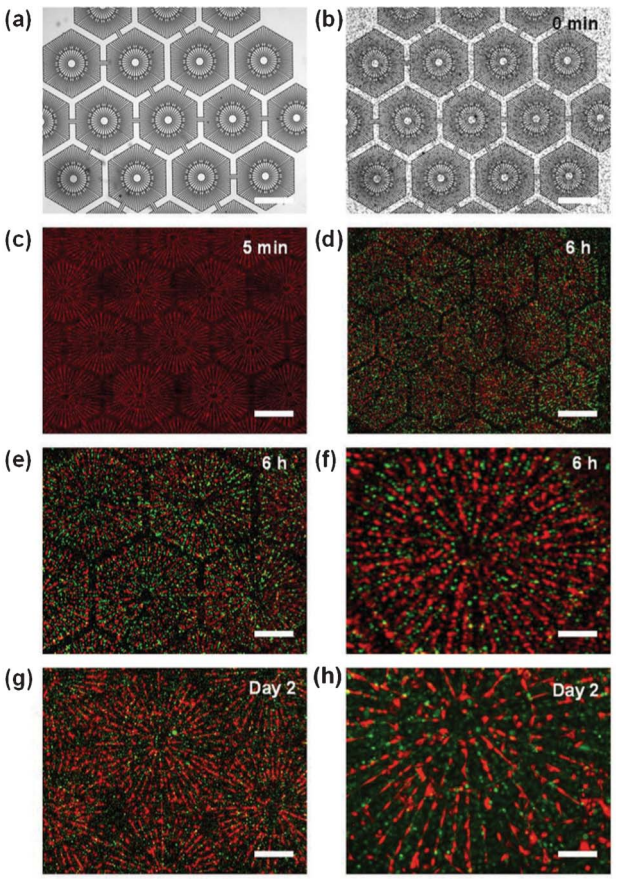

Fig. 6 On-chip heterogeneous-integration demonstration of liver cells (HepG2 cells, red fluorescence) and endothelial cells (HUVECs, green fluorescence) *via* lobule-mimetic DEP cell patterning. (a) and (b) show the top-view pictures above the cell-patterning area, before and after the HepG2 cells were loaded into the area above the cell patterning electrodes, respectively. (c) After the first DEP patterning by applying an AC potential of 5 V_{pk-pk} at 1 MHz, the HepG2 cells were micropatterned onto the inner lobule-mimetic-stellate electrode array to form the HepG2-cells-assembled pattern of multiple radial lines. (d) After six hours culturing, the micropatterned HepG2 cells were firmly adhered in place. Then, the second DEP force was applied to pattern the HUVECs at the position of the outer lobule-mimetic-stellate electrodes array to form heterogeneous integration of lobule-mimetic patterning to achieve the *in vitro* centimetre-scale reconstruction of complex lobule-mimetic liver tissue. (e) The zoom-in view of (d) shows six lobule-mimetic modules. (f) The zoom-in view of (e) shows a single lobule-mimetic module. (g) After two days incubation with the DEP force off, the patterned HepG2 cells were maintained in place and grew well. (h) The zoom-in view of (g). Scale bar: (a–d) 1.5 mm, (e, g) 700 μm, (f, h) 100 μm.

HepG2 cells were loaded into the area above the cell patterning electrodes, respectively. After applying an external AC signal of 5 V_{pk-pk} at 1 MHz between the top ITO ground electrode and the bottom 1st inner lobule-mimetic cell patterning electrode for the vertical positive DEP operation, the spatial non-uniform electric field gradient was generated to guide, snare and micropattern the HepG2 cells to form the HepG2-cells-assembled pattern of multiple radial lines [Fig. 6(c)]. Next, after a step-by-step medium regulation process from sugar buffer to culture medium for enhancing the cell-to-substrate adhesion and culturing the HepG2 cells for six hours, during the six-hour culturing, the DEP voltage was turned off. Then the second type of endothelial cells (HUVECs) were loaded in. Then an AC potential of 5 V_{pk-pk} at 1 MHz was applied again between the top ITO ground electrode and the bottom 2nd outer patterning electrode. The location of the 2nd outer lobule-mimetic cell patterning electrode array provided the local electric-field maximum and functionally acted as the starting point of primer for capturing the field-guiding HUVECs. Plenty of HUVECs were in-parallel guided, positioned and trapped onto the energized cell patterning electrodes. Now HepG2-cells formed multiple radial lines interlaced with the HUVECs of multiple radial lines, which achieved the *in vitro* centimetre-scale reconstruction of complex lobule-mimetic liver tissue [Fig. 6(d)]. For our present chip design, tens of thousands of HepG2 cells could be snared and positioned to achieve a single lobule-mimetic module with a 2D patterning region of about 2 mm^2 in each. Fig. 6(d) shows the large area lobule-mimetic reconstruction with nineteen lobule-mimetic modules. Fig. 6(e) shows the local enlarged view of Fig. 6(d) with six lobule-mimetic modules. Fig. 6(f) shows a single lobule-mimetic module consisting of the precise pattern of multiple radial hepatic cell-strings interlaced in-between the multiple radial endothelial cell-strings with single cell resolution. We did not observe any significant problem about the non-specific spreading of HepG2 cells beyond their patterned electrode. The heterogeneous integration *via* our liver-cell patterning labchip design exhibited a significant lobule-mimetic pattern with the patterning resolution enhancement to single cell to provide an intimate contact for cell-to-cell and cell-to-ECM interactions during cellular development.

After a two-day incubation with the DEP force off, the patterned HepG2 cells were maintained in place and grew well. In some regions, two adjacent patterned HepG2 cells were merged into one cellular unity, while somewhere there were more than three or four cells intimately contacted to form a cell group [Fig. 6(g) and (h)]. Most HepG2 cells adhered to the substrate and elongated their body *via* spreading their cytoskeleton along the lobule-mimetic-stellate electrodes to form the multiple radial line patterns array. Most HUVECs grew well in place and normally adhered to the substrate with little morphological changes, whiles some HUVECs adhered to the substrate *via* elongating their body along the lobule-mimetic-stellate electrodes. Besides, some patterned HepG2 cells and HUVECs proliferated and grew into colonies while some of them presented their motility and crawled to the vicinity. All these behaviors of cell adhesion/spreading/growth imply that the DEP-patterned HepG2 cells and HUVECs were not only viable but also revealed their physiological behavior such as cell proliferation, cell–cell/cell–ECM interactions and cell migration. Fig. 7 shows a close side view of repeated radiating liver patterns with dense heterogeneous integration and cell-to-cell interactions. The alternate radiating patterned endothelial cells mimic the shape and the function of sinusoid-like vascular endothelial lining cells that are shown in the classic real hepatic lobule.

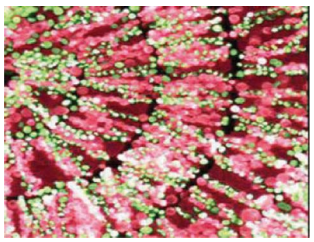

Fig. 7 The zoom-in side view of repeated radiating liver pattern, as shown in Fig. 6(h), with dense heterogeneous integration and cell-to-cell interaction.

Engineered-liver function assessment *via* CYP450-1A1 enzyme activity

CYP450-1A1 enzyme activity is a liver-specific function which can be used to quantitatively assess the drug metabolism of liver cells. CYP450-1A1 enzyme activity increases with the concentration of β-naphthoflavone (0–20 μM) after a 48 h induction. The maximum induction of CYP450-1A1 enzyme activity was observed at 10 μM β-naphthoflavone, which strongly induced the activity by about 5 times. In our experiments, cell culture medium was replaced with the fresh medium containing the specific CYP450-1A1 inducer β-naphthoflavone (final concentration 10 μM; Sigma-Aldrich) daily and the cells were incubated for 48 h. After 48 h, the medium was removed and the cells were washed twice with PBS and serum-free medium containing 10 μM ethoxyresorufin (Sigma-Aldrich), along with 25 μM dicumarol (Sigma-Aldrich) to prevent subsequent metabolism of resorufin. After a further 60 min of incubation, the cell culture supernatants were collected and pipetted into black 96-well plates (Nunc, Denmark). The fluorescence intensities of resorufin were determined at em/ex 530/595 nm by using Wallac 1420 VICTOR2 multilabel plate readers (Perkin-Elmer, Waltham, Massachusetts) and calibrated by the total cell number of HepG2.

Fig. 8 shows CYP450-1A1 enzyme activity measurements for non-patterned HepG2, patterned pure HepG2, non-patterned co-cultured cells (HepG2+HUVECs) and (lobule-mimetic) engineered/patterned cells (HepG2+HUVECs) under the culturing conditions of 2 h and 2 days. It shows interesting results. The patterned pure HepG2 showed higher CYP450-1A1 enzyme activity than the non-patterned pure HepG2 after a 2-day culture. From the observations of Fig. 4(e) and (g), the patterned HepG2 cells adhered and spread onto the substrate to form a radial shaped line array of lobule-mimetic pattern. Also, most of the patterned HepG2 cells adhered and elongated their body along the place of the lobule-mimetic-stellate electrode [Fig. 4(e)]. It will be interesting for further

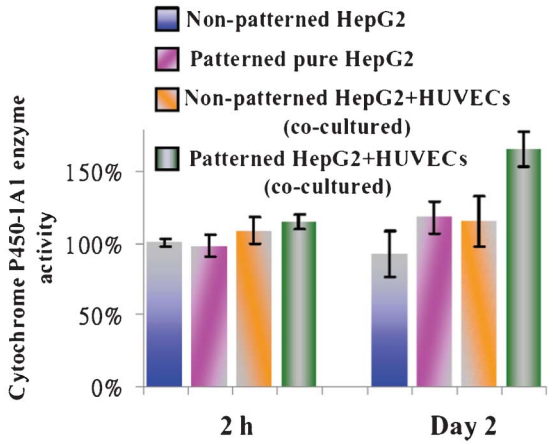

Fig. 8 CYP450-1A1 enzyme activity comparison for non-patterned HepG2, patterned HepG2, non-patterned co-cultured cells (HepG2+HUVECs) and (lobule-mimetic) engineered/patterned cells (HepG2+HUVECs) under the conditions of culturing for 2 h and 2 days. Each data bar represents the mean of 5 samples.

studies to be undertaken on whether there is any coherence or not between the liver function (CYP450-1A1 enzyme activity) and the phenomenon observed in Fig. 4(e) and (g). Under 2-day co-culture conditions, the engineered/patterned cells (HepG2+HUVECs) showed higher CYP450-1A1 enzyme activity than non-patterned HepG2, patterned HepG2 and non-patterned co-cultured cells (HepG2+HUVECs) [Fig. 8]. It was revealed that the CYP450-1A1 enzyme activity on engineered/patterned cells (HepG2+HUVECs) was 80%, 41% and 43% higher than the non-patterned pure HepG2, patterned pure HepG2 and non-patterned co-cultured cells (HepG2+HUVECs), respectively, after a 2-day culture. CYP450-1A1 enzyme activity was significantly ($P < 0.01$) enhanced in the patterned co-culture (HepG2+HUVECs).

Further studies on cell–cell interaction, growth, drug tests, and 3-D cell patterning are on-going in our group. Appropriate micropatterning of HepG2 cells and HUVECs to establish large-area units of the liver lobule would not only benefit the fundamental study of liver tissue but also is the key step towards functional liver tissue engineering. The forward evolution of this technique demonstrated here could be promisingly applied to the fields of tissue engineering, drug development and liver physiology studies.

Conclusion

A fine cell patterning technique capable of manipulating heterogeneous cell types, providing high resolution patterns and preserving cell-to-cell interactions is crucial and important toward functional artificial liver in tissue engineering. In this paper, we demonstrated a DEP-based liver cell patterning technique capable of rapidly and on-chip reconstruction of the heterogeneous lobule-mimetic liver tissue *via* our specific lobule-mimetic-stellate-electrodes design. The original and millions of randomly distributed hepatic and endothelial cells could be in-parallel manipulated *via* field-induced DEP force to form a large area array of a lobule, consisting of the radial and interlaced pattern of hepatic–endothelial cell-strings, with high patterning resolution, centimetre-scale pattern and high cell viability. The liver function was investigated by examining CYP450-1A1 enzyme activity. The enhancement of CYP450-1A1 enzyme activity for our engineered liver tissue was demonstrated. In this paper, the field-induced DEP force was generated *via* fixed electrodes on the substrate glass. In our group, we are also developing electrodeless DEP manipulation for cells *via* optoelectronic dielectrophoresis[42] as well as poly(ethylene) glycol diacrylate (PEGDA) gel techniques to extend the applications.

Acknowledgements

This research is supported by National Science Council of Taiwan, under the grant NSC 99-2120-M-007-001.

References

1 R. Langer and P. J. Vacanti, Tissue Engineering, *Science*, 1993, **260**, 920–926.
2 U. A. Stock and J. P. Vacanti, Tissue engineering: current state and prospects, *Annu. Rev. Med.*, 2001, **52**, 443–451.
3 L. G. Griffith and G. Naughton, Tissue engineering: current challenges and expanding opportunities, *Science*, 2002, **295**, 1009–1014.
4 J. W. Allen and S. N. Bhatia, Engineering Liver Therapies for the Future, *Tissue Eng.*, 2002, **8**(5), 725–737.
5 H. Andersson and A. van den Berg, Microfabrication and microfluidics for tissue engineering: state of the art and future opportunities, *Lab Chip*, 2004, **4**, 98–103.
6 A. S. Rudolph, Cell and tissue based technologies for environmental detection and medical diagnostics, *Biosens. Bioelectron.*, 2001, **16**, 429–431.
7 W. M. Saltzman and W. L. Olbricht, Building Drug Delivery into Tissue Engineering, *Nat. Rev. Drug Discovery*, 2002, **1**, 177–186.
8 K. Bhadriraju and C. S. Chen, Engineering cellular microenvironments to improve cell-based drug testing, *Drug Discovery Today*, 2002, **7**(11), 612–620.
9 A. Khademhosseini, R. Langer, J. Borenstein and J. P. Vacanti, Microscale technologies for tissue engineering and biology, *Proc. Natl. Acad. Sci. U. S. A.*, 2006, **103**(8), 2480–2487.
10 D. W. Huntmacher, Scaffold design and fabrication technologies for engineering tissues-state of the art and future perspectives, *J. Biomater. Sci., Polym. Ed.*, 2001, **12**(1), 107–124.
11 V. L. Tsang and S. N. Bhatia, Three-dimensional tissue fabrication, *Adv. Drug Delivery Rev.*, 2004, **56**, 1635–1647.
12 R. S. McCuskey, Morphological mechanisms for regulating blood flow through hepatic sinusoids, *Liver Int.*, 2000, **20**, 3–7.
13 S. R. Khetani and S. N. Bhatia, Microscale culture of human liver cells for drug development, *Nat. Biotechnol.*, 2008, **26**, 120–126.

14 M. Mrksich, L. E. Dike, J. Tien, D. E. Ingber and G. M. Whitesides, Using microcontact printing to pattern the attachment of mammalian cells to self-assembled monolayers of alkanethiolates on transparent films of gold and silver, *Exp. Cell Res.*, 1997, **235**, 305–313.
15 D. T. Chiu, N. L. Jeon, S. Huang, R. S. Kane, C. J. Wargo, I. S. Choi, D. E. Ingber and G. M. Whitesides, Patterned deposition of cells and proteins onto surfaces by using three-dimensional microfluidic systems, *Proc. Natl. Acad. Sci. U. S. A.*, 2000, **97**(6), 2408–2413.
16 V. Mironov, T. Boland, T. Trusk and G. Forgacs, *et al.*, Organ printing: computer-aided jet-based 3D tissue engineering, *Trends Biotechnol.*, 2003, **21**, 157–161.
17 Y. Nahmias, R. E. Schwartz, C. M. Verfaillie and D. J. Odde, Laser-guided direct writing for three-dimensional tissue engineering, *Biotechnol. Bioeng.*, 2005, **92**(2), 129–136.
18 H. Tavana, B. Mosadegh and S. Takayama, Polymeric aqueous biphasic systems for non-contact cell printing on cells: engineering heterocellular embryonic stem cell niches, *Adv. Mater.*, 2010, **22**(24), 2628–2631.
19 H. Tavana, B. Mosadegh, P. Zamankhan, J. B. Grotberg and S. Takayama, Microprinted feeder cells guide embryonic stem cell fate, *Biotechnol. Bioeng.*, 2011, **108**(10), 2509–2516.
20 C.-T. Ho, R.-Z. Lin, W.-Y. Chang, H.-Y. Chang and C.-H. Liu, Rapid heterogeneous liver-cell on-chip patterning via the enhanced field-induced dielectrophoresis trap, *Lab Chip*, 2006, **6**, 724–734.
21 H. A. Pohl, *Dielectrophoresis*, Cambridge University Press, Cambridge, UK, 1978.
22 M. P. Hughes, *Nanoelectromechanics in Enginnering and Biology*, CRC Press, Boca Raton, 2003.
23 N. G. Green, H. Morgan and J. J. Milner, Manipulation and trapping of sub-micro bioparticles using dielectrophoresis, *J. Biochem. Biophys. Methods*, 1997, **35**, 89–102.
24 T. Muller, G. Gradl, S. Howitz, S. Shirley, T. Schnelle and G. Fuhr, A 3-D microelectrode system for handling and caging single cells and particles, *Biosens. Bioelectron.*, 1999, **14**, 247–256.
25 S.-M. Yang, T.-M. Yu, H.-P. Huang, M.-Y. Ku, L. Hsu and C.-H. Liu, Dynamic manipulation and patterning of microparticles and cells by using TiOPc-based optoelectronic dielectrophoresis, *Opt. Lett.*, 2010, **35**(12), 1959.
26 H. Morgan, M. P. Hughes and N. G. Green, Separation of subparticles by dielectrophoresis, *Biophys. J.*, 1999, **77**, 516–525.
27 S. Choi and J. K. Park, Microfluidic system for dielectrophoretic separation based on a trapezoidal electrode array, *Lab Chip*, 2005, **5**, 1161–1167.
28 S. Fiedler, S. G. Shirley, T. Schnelle and G. Fuhr, Dielectrophoretic sorting of particles and cells in a microsystem, *Anal. Chem.*, 1998, **70**, 1909–1915.
29 J. H. Nieuwenhuis, A. Jachimowicz, P. Svasek and M. J. Vellekoop, Optimization of microfluidic particles sorters based on dielectrophoresis, *Sensors Journal*, 2005(8), 810–816.
30 S.-M. Yang, P. T. Harishchandra, T.-M. Yu, M.-H. Liu, L. Hsu and C.-H. Liu, Concentration of magnetic beads utilizing light-induced electroosmosis flow, *IEEE Trans. Magn.*, 2011, **47**(10), 2418–2421.
31 J. Lu, C. A. Barrios, A. R. Dickson, J. L. Nourse, A. P. Lee and L. A. Flanagan, Advancing practical usage of microtechnology: a study of the functional consequences of dielectrophoresis on neural stem cells, *Integr. Biol.*, 2012, **4**(10), 1223–1236.
32 S. V. Puttaswamy, S. Sivashankar, C.-H. Yeh, R.-J. Chen and C. H. Liu, Enhanced cell viability and cell adhesion using low conductivity medium for negative dielectrophoretic cell patterning, *Biotechnol. J.*, 2010, **5**(10), 1005–1015.
33 D. S. Gray, J. L. Tan, J. Voldman and C. S. Chen, Dielectrophoretic registration of living cells to a microelectrode array, *Biosens. Bioelectron.*, 2004, **19**, 771–780.
34 D. R. Albrecht, V. L. Tsang, R. L. Sah and S. N. Bhatia, Photo- and electropatterning of hydrogel-encapsulated living cell array, *Lab Chip*, 2005, **5**, 111–118.
35 B. Alp, J. S. Andrews, V. P. Mason, I. P. Thompson, R. Wolowacz and G. H. Markx, Building structured biomaterials using AC electrokinetics, *IEEE Eng. Med. Biol. Mag.*, 2003, 91–97.
36 R. Pethig, Dielectrophoresis: using inhomogeneous AC electrical fields to separate and manipulate cells, *Crit. Rev. Biotechnol.*, 1996, **16**, 331.
37 T. B. Jones, Basic Theory of Dielectrophoresis and Electrorotation, *IEEE Engineering in Medicine Biology Magazine*, Nov. 2003, 33–42.
38 E. A. Jaffe, R. L. Nachman, C. G. Becker and C. R. Minick, Culture of human endothelial cells derived from umbilical veins, identification by morphologic and immunological criteria, *J. Clin. Invest.*, 1973, **52**, 2745–2756.
39 M. D. Burke and R. T. Mayer, Ethoxyresorufin: Direct fluorimetric assay of a microsomal O-dealkylation which is preferentially inducible by 3-methylcholanthrene, *Drug Metab. Dispos.*, 1974, **2**, 583–588.
40 T. Matsushita, K. Nakano, Y. Nishikura, K. Higuchi, A. Kiyota and R. Ueoka, Spheroid formation and functional restoration of human fetal hepatocytes on poly-L-amino acid-coated dishes after serial proliferation, *Cytotechnology*, 2003, **42**, 57–66.
41 R. A. Lubet, R. W. Nims, R. T. Mayer, J. W. Cameron and L. M. Schechtman, Measurement of cytochrome P-450 dependent dealkylation of alkoxyphenoxazones in hepatic S9s and hepatocyte homogenates: effects of dicumarol, *Mutat. Res.*, 1985, **142**, 127–131.
42 S.-M. Yang, T.-M. Yu, H.-P. Huang, M.-Y. Ku, L. Hsu and C.-H. Liu, Dynamic manipulation and patterning of microparticles and cells by using TiOPc-based optoelectronic dielectrophoresis, *Opt. Lett.*, 2010, **35**(12), 1959.